IEEE Access
Multidisciplinary ⋮ Rapid Review ⋮ Open Access Journal

Received December 28, 2020, accepted February 7, 2021, date of publication February 24, 2021, date of current version March 5, 2021.

Digital Object Identifier 10.1109/ACCESS.2021.3062085

Wi-Fi RTT-Based Active Monopulse RADAR for Single Access Point Localization

JOSÉ ANTONIO LÓPEZ-PASTOR[1], (Graduate Student Member, IEEE), PEDRO ARQUES-LARA[2], JUAN JOSÉ FRANCO-PEÑARANDA[2], ANTONIO JAVIER GARCÍA-SÁNCHEZ[3], AND JOSÉ LUIS GÓMEZ-TORNERO[3], (Senior Member, IEEE)

[1]Marketing Activo Inteligente, SL (Neuromobile), 30100 Murcia, Spain
[2]Centro Tecnológico TIC (CENTIC), 30100 Murcia, Spain
[3]Department of Communication and Information Technologies, Technical University of Cartagena (UPCT), 30202 Cartagena, Spain

Corresponding author: José Antonio López-Pastor (jlopez@neuromobilemarketing.com)

This work was supported in part by the Spanish National Project under Grant PID2019-103982RB-C42/AEI/10.13039/501100011033, in part by the Ministerio de Ciencia e Innovación de España (MICINN) under Grant DIN2018-009815, in part by the Murcia Regional Projects under Grant INFO 2018.08.ID+I.0015 and Grant 2020.08.CT01.0024, in part by the ATENTO Project (Fundación Séneca, Región de Murcia), under Grant 20889/PI/18, and in part by the LIFE Project (Fondo SUPERA Covid-19 funded by Consejo Superior de Investigaciones Científicas CSIC, Universidades Españolas, and Banco Santander).

ABSTRACT The purpose of this work is to implement a novel active radar system for single access point two-dimensional localization system based on 802.11 wireless local-area networks (WLAN). The active radar employes the 802.11 Fine Time Measurement (FTM) Round Trip Time (RTT) as specified in the 2016 update of WIFI Standard to calculate the ranging distance and acquires two channels of Received Signal Strength Indicator (RSSI) to estimate the azimuthal angle. In this way, real-time two-dimensional localization of Wi-Fi RTT-compatible mobile Internet of Things devices is demonstrated using a single access point operating in the 2.4GHz band. The experimental results performed in anechoic chamber and in a real environment point up a mean positioning error below one meter within a Field of View (FoV) of 60° and distances up to 14 meters, with an acquisition time below 0.5 seconds.

INDEX TERMS Localization with 802.11, active Wi-Fi radar, round trip time (RTT), angle of arrival (AoA), amplitude monopulse radar.

I. INTRODUCTION

Real-timelocalization systems (RTLS) is one of the key enabling technologies for efficient Internet of Things (IoT) applications and services [1]. More particularly, RTLS for mobile devices connected to wireless local-area networks (WLAN) based on the globally spread 802.11 Wi-Fi protocols have been widely proposed [2] as an indoor localization option when the Global Navigation Satellite System (GNSS) cannot be precisely employed. Regarding indoor environments, RTLS can be divided into fingerprinting (FP), Time of Arrival (ToA), and Angle of Arrival (AoA). In the last years, FP has been one of the most predominant indoor location techniques [3]–[5] because every Wi-Fi card adapter provides RSSI values. The main drawback of this technique is that they rely on an extensive and time-consuming off-line calibration phase [6] and the variations over the time of fingerprint in a large building require periodic recalibrations [7]. ToA ranging methods require at least three Access Points (APs) for triangulation techniques, and it can be based on Received Signal Strength Information (RSSI) [8], [9], or on the measure of the time-of-flight of the communications accessing by the Channel State Information (CSI) [10] of the Wi-Fi card. This technique, widely used in high-bandwidth location systems like UWB, has the handicap of lower performance in a higher multipath environment [11]. Moreover, a small error in the time measures causes a significant error in the computed distance because of the speed of light. For this reason, CSI-based techniques require complex calibration for synchronization and/or modifying the hardware/software to acquire complex CSI / IQ data to obtain Time-of-Fligth information. The estimation of AoA usually requires to employ array antenna systems [12] along with complex signal processing techniques [13], [14] where the IQ information from

The associate editor coordinating the review of this manuscript and approving it for publication was Wei Liu.

the signal is involved. However, another approach to estimate AoA from accessible RSSI data can be found in the literature [15], [16].

Furthermore, related to the ToA location techniques for smartphones devices, a new scenario has been established with the adoption of the 802.11mc (Wi-Fi Fine Time Measurement, FTM) standard [17] by the Android smartphone Android 9 and higher releases [18]. According to the Wi-Fi Alliance, an accuracy in meters' level can be reached with this standard employing the Round-Trip-Time (RTT) procedure. A complete empirical analysis of the FTM protocol was performed in [19], and in [20], [21] location systems employing RTT and inertial sensors from smartphones are depicted.

All the aforementioned works required several APs to localize IoT devices. In most cases, the higher the number of APs, the better the accuracy of the systems. Nevertheless, in the IoT paradigm, under some premises such as smart-connected home [22], only one single or few APs are available to implement services based on the precise ubication of the inhabitants of the home.

In this context, several two-dimensional localization systems based on a single Wi-Fi AP can be found in the scientific literature. To the best of our knowledge, CUPID [23] is the first proposal of a single-AP indoor location algorithm using commodity APs. The position of a smartphone employing CUPID is determined by a combination of ranging and AoA obtained by accessing to CSI. An improved version from the same authors of CUPID is SAIL [24]. In this work, the range estimations are based on the use of ToF computed by accessing to CSI together with a dead reckoning system based on a Kalman Filter implemented on Android smartphones. Another single AP location ToF-based algorithm is Chronos [25]. It reaches decimeters accuracy employing MIMO (Multiple-Input Multiple-Output) two antennas commercial devices. This accuracy in the ToF estimation is achieved with the implementation of channel hopping and combining the 35 different frequency bands as a wideband radio. The implementation requires driver modification of the Wi-Fi card driver for the channel hopping, and it is out of the Wi-Fi standard. Similar to Chronos, the S-Phaser implementation [26] is a frequency hopping system. Nonetheless, it only uses two different channels. In detail, S-Phaser employs CSI data and a proposed Interpolation Elimination Method (IEM) to remove the phase and angle error of the direct path of the signal. Afterward, it implements the Broadband Angle Ranging (BAR) to determine the transmitter distance and triangulation techniques to determine the location.

Another ToF related to single AP work is SiFi [27]. It utilizes a three-antennas MIMO single channel and a single AP indoor location protocol built with commodity hardware. As opposed to [23], [24], SiFi does not require extra information from smartphone sensors. However, it requires access simultaneously to the CSI of the three antennas of the MIMO Wi-Fi card during the communication and cannot be employed in real-time applications due to the latency of the Linux CSI Tool and the computation complexity. Another key drawback is that only one device can be located at a time. Splicer [28] is also in the bucket of CSI single AP location system. It is based on the power delay profiling of the CSI measures and can be implemented with only one commodity Wi-Fi AP. The algorithm needs collecting the CSI of several packets at different frequencies. Thereby, channel hopping method is required. With the power delay profile system, the ranging to the devices can be precisely computed.

Some other works implement single AP indoor location systems using directly accessible RSSI, thus avoiding the need of CSI data. The work [29] employs Switched Beam Antenna (SBA) with eight dual Wi-Fi directional antennas to implement a simultaneous range together with AoA system with the RSSI. Similarly, in [30], RSSI data collected from a SBA is used in conjunction with motion sensors to compute the precise location. Therefore, all previous single AP Wi-Fi localization systems are developed according the bases of signal processing, which in turn integrates complex CSI acquisition / phased-array techniques [23]–[28], or on more straightforward RSSI processing at the cost of using complex electronically switchable antenna arrays [29]–[30].

The main contribution of this work is the demonstration for the first time of the conception of a simple active RADAR for Wi-Fi RTLS using a single access point (AP), which does not require complex CSI data or expensive phased-array / switched beam antennas. This digital radar is conceived under the premises of the 802.11mc RTT protocol to estimate the range distance and a monopulse antenna to estimate the azimuthal angle from the measured RSS (Received Signal Strength) levels. To the best of our knowledge, this is the first work where both technologies have been combined for location purposes. Section II describes this digital Wi-Fi RTT monopulse RADAR, and its calibration phase in the anechoic chamber is detailed in Section III. The real-time two-dimensional localization performance in an outdoor scenario is evaluated in Section IV, showing a mean positioning error below 1 meter within a Field of View of 60° and distances up to 14 meters, with an acquisition time below 0.5 seconds. Finally, Section V compares this active Wi-Fi RADAR with other single access point Wi-Fi RTLS proposals described in the literature and, finally, summarizes the main conclusions of this work and future lines to improve this innovative IoT indoor localization system.

II. WI-FI RTT MONOPULSE SYSTEM DESCRIPTION

Classical monopulse RADAR systems have been used for decades to estimate the range distance and angular location of mobile objects from the received echoes [31]. More recently, MIMO RADAR systems are being developed for passive target tracking [32]. Our novel monopulse Wi-Fi system is based on this concept, and can be understood as an active digital version of classical passive monopulse RADAR. It is an active RADAR since the range distance is not measured from the passive reflection of transmitted echoes, but on active communication using 802.11mc Wi-Fi Fine Time Measurement (FTM) standard [17]. This FTM standard allows

digital Round-Trip-Time (RTT) measurements, which would be equivalent to the analog radio-frequency (RF) echo two-way travel time, from which the range distance R can be calculated with a meters' level accuracy [19]–[21]. In addition, the Wi-Fi RSSI-based monopulse technique proposed in [15], [16] can be used to estimate the azimuthal bearing angle ϕ associated to the Direction-of-Arrival (AoA). Therefore, range R and AoA angle ϕ estimation based on active digital Wi-Fi metrics (RTT and RSSI, respectively) are combined, and once the distance and the angle are obtained, the precise (x,y) position can be directly computed as in analog RF microwave monopulse RADAR.

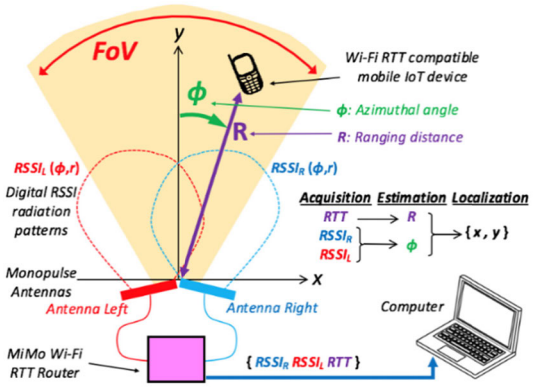

FIGURE 1. Scheme of the proposed Wi-Fi RTT active monopulse RADAR.

The scheme of the system is illustrated in Fig.1, showing a single 2 × 2 MIMO 802.11mc Wi-Fi AP which is connected to two antennas (namely antenna left and right) in tilted monopulse configuration [16]. As previously described, by communicating with a RTT-compatible mobile device, the RTT and the RSSI acquired by each antenna are processed in a personal computer to estimate the range distance R and the azimuthal AoA ϕ, and eventually the 2D position {x,y}, as also illustrated in Fig. 1.

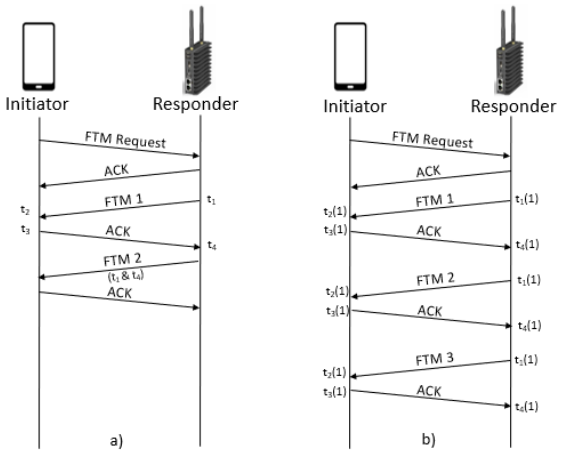

FIGURE 2. 802.11mc fine time measurement (FTM) protocol for RTT acquisition.

Regarding the 802.11mc standard to obtain the RTT, it is based on the FTM protocol [17]. This is a device-to-device location protocol that requires that an initiator (in our case a smartphone, but it can be any other IoT device) asks for a ranging request to a responder, which is a Wi-Fi AP. The protocol is illustrated in Fig.2. The first message frame sent by the initiator to the responder is labeled as FTM request. When the request is received by the responder, it dispaches an acknowledge (ACK) frame to the initiator. This initiates an exchange of two FTM-ACK frames from which the RTT can be calculated from the associated timestamps t_1, t_2, t_3 and t_4 summarized in Fig. 2a, following the next relation:

$$RTT = \frac{(t_4 - t_1) - (t_3 - t_2)}{2} \tag{1}$$

This process can be repeated as a burst of n RTT-ACK frames, as shown in Fig. 2b, to increase the RTT estimation accuracy as follows:

$$RTT = \frac{1}{n}\left(\sum_{k=1}^{n} t_4\,(k) - \sum_{k=1}^{n} t_1\,(k)\right) - \frac{1}{n}\left(\sum_{k=1}^{n} t_3\,(k) - \sum_{k=1}^{n} t_2\,(k)\right) \tag{2}$$

For each of the FTM requests from an initiator, the above protocol has to be executed. Once the RTT is computed, the range R is estimated by multiplicating the time by the speed of light c_0 and applicating a correction factor R_{OFFSET} which must be calibrated a priori [19]:

$$R = RTT/2 \cdot c_0 + R_{OFFSET} \tag{3}$$

This result is obtained by the initiator without the requirement of being connected to the AP, and it is implemented in Android via API. This is an easy-to-use already available technology present in commodity APs and mobile devices which are compatible with the 802.11mc standard, in contrast to less accessible Time-of-Flight estimation based on hardware modification for AP synchronization or CSI acquisition [23]–[28]. In our case, we use a Yocto Wild AP [33] equipped with a MIMO Wi-Fi chipset Intel 8260AC as the FTM-compatible responder. As initiator, we use an Asus Rog Phone II with the Qualcomm® Snapdragon™ 845, which is a 802.11mc compatible smarphone. They are shown in the picture of Fig.3.

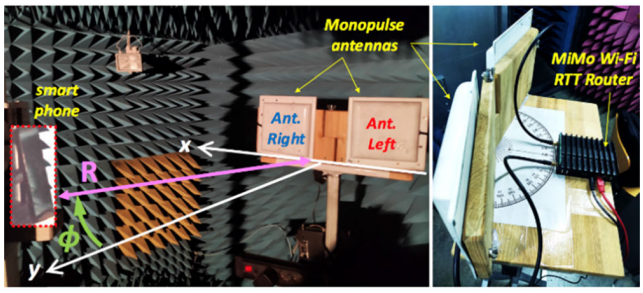

FIGURE 3. Picture of Wi-Fi RTT active monopulse RADAR in anechoic chamber.

Regarding the estimation of the azimuthal AoA angle ϕ, the monopulse power-based technique [31], [32] employing two tiled antennas, has recently demonstrated a good estimation of the AoA for Wi-Fi low-cost systems [16]. Its main advantage, when compared to other Wi-Fi AoA techniques applying complex CSI data for AoA estimation [23]–[28], is that directly accessible RSSI data is used for the AoA processing. In our case, we connect the MIMO Wi-Fi AP to two commercial panel antennas [34], which are as antenna left and antenna right in the scheme of Fig.1, and they are also depicted in the picture of Fig.3.

The monopulse technique is based on the different power levels received at each one of the two tilted antennas, depending on the azimuthal ϕ AoA of the Wi-Fi signal emitted by the device. With the RSSI measured by each antenna as a function of the incoming angle ϕ, the sum (Σ) and difference (Δ) patterns are generated. Besides, it must be taken into account that smartphone localization using Wi-Fi systems can operate in the near-field radiation region of the monopulse antennas [35], and therefore the monopulse function must be calibrated for different radial distances R inside this near-field zone, and also for the far-field region. The monopulse function $\Psi = \Delta/\Sigma(\phi,R)$ is defined in expression (4), where $K_D(R)$ is a correction factor which must be calibrated as a function of distance [35].

$$\Psi(\phi,R) = \frac{\Delta(\phi,R)}{\Sigma(\phi,R)} = \frac{RSSI_R(\phi,R) - K_D(R)\cdot RSSI_L(\phi,R)}{RSSI_R(\phi,R) + K_D(R)\cdot RSSI_L(\phi,R)} \tag{4}$$

To estimate the AoA angle ϕ, the RSSI acquired by each antenna of the MIMO AP is read and the monopulse value Ψ_{RSSI} is calculated in (5). Then a direct numerical search is performed to obtain the estimated AoA ϕ_{EST} which minimizes the monopulse comparison error function defined in equation (6):

$$\Psi_{RSSI} = \frac{\Delta_{RSSI}}{\Sigma_{RSSI}} = \frac{RSSI_R - K_D \cdot RSSI_L}{RSSI_R + K_D \cdot RSSI_L} \tag{5}$$

$$DoA = \phi_{EST} \overset{yields}{\longrightarrow} min\,|\Psi(\phi_{EST},R) - \Psi_{RSSI}| \tag{6}$$

III. RANGING AND ANGULAR CALIBRATION

As described, both the RTT estimation (1)-(3) and the AoA estimation (4)-(6), need a calibration phase before the estimation process can be initiated. This calibration is performed in an anechoic chamber as shown in Fig.3, which allows to measure angular radiation patterns as a function of the distance between R = 50cm and R = 3m.

The calibration steps are sketched in Fig.4. First, the offset R_{OFFSET} in equation (3) must be calibrated to carry out accurate evaluation of the RTT and thus precise estimation of the ranging distance R. For that, the RTT is measured in the anechoic chamber as a function of the radial distance R and for different angular directions ϕ. The experiments have been performed in channel #6 (2.437 GHz) with a 20MHz bandwidth. The measurements are depicted in Fig.5. This figure shows an offset R_{OFFSET} = 600cm is the more suitable

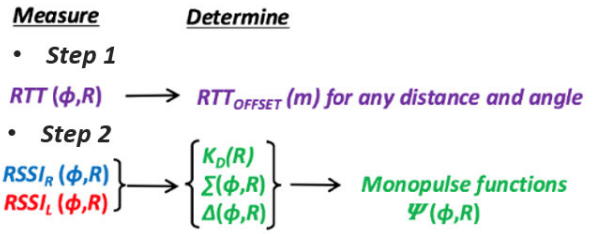

FIGURE 4. Steps in the calibration process.

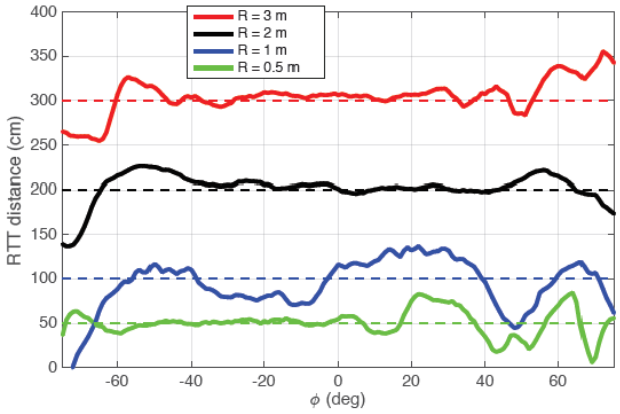

FIGURE 5. Measured ranging distance R after calibration of the RTT offset.

for all the ranging distances from R = 50cm to R = 3m. As can be seen, the estimated RTT ranging error is more significant for shortest distances R = 1m and R = 50cm. Also, it can be observed that the estimation error increases for angles of observation higher than $\phi = \pm 60°$. As will be shown, this is related to the Field of View (FoV) of the monopulse antennas, which gain strongly decreases out of this angular zone. In any case, the calibrated RTT offset is established to the fixed value R_{OFFSET} = 600cm, as summarized in Table 1. This fixed value must be *independent* of the unknown distance R and AoA angle ϕ, since it will be used to estimate the ranging R and the AoA direction ϕ.

The next step is to calibrate the monopulse functions as a function of the ranging distance R and the azimuthal angle ϕ, following equations (4)-(6). To this end, the digital sum $\Sigma(\phi, R)$ and difference $\Delta(\phi, R)$ patterns shown in Fig.6 are characterized by acquiring the RSSI levels at the left and right antennas, which in turn depend on the azimuthal angle and the ranging distance R.

The measured normalized RSSI angular patterns are plotted in Fig.6 for the same ranging distances from R = 50 cm to R = 3m as in Fig.5. As described in [35], the angular patterns vary due to the near-field effects, and this must be considered for accurate angular estimation in short distances. In our case, the near-field zone reaches up to R = 2.5 m; for larger distances the far-field patterns obtained for R = 3 m can be used. Similarly, the correction factor $K_D(R)$ in (4) must be properly calibrated for distances in the near-field zone, in order to obtain accurate monopulse functions. The values

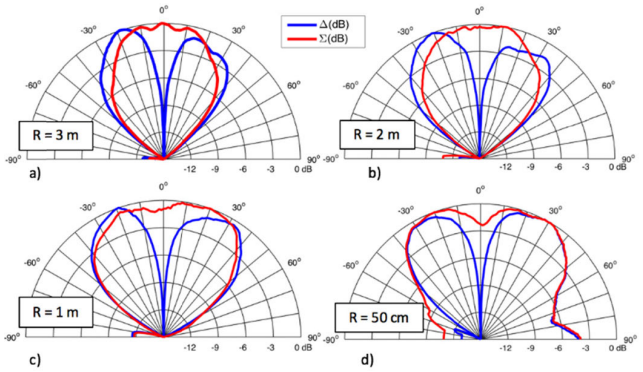

FIGURE 6. Measured sum and difference patterns as a function of ranging distance R after calibration of the monopulse offset.

TABLE 1. Calibration of RTT Offset R_{OFFSET} and Monopulse Factor K_D.

Distance R (m)	R_{OFFSET} (cm)	K_D (dB)
3	600	-0.7
2	600	-1.0
1	600	-2.3
0.5	600	-4.0

of $K_D(R)$ to obtain the optimum calibrated normalized RSSI patterns in Fig.6 as function of the ranging distance R, are summarized in Table 1.

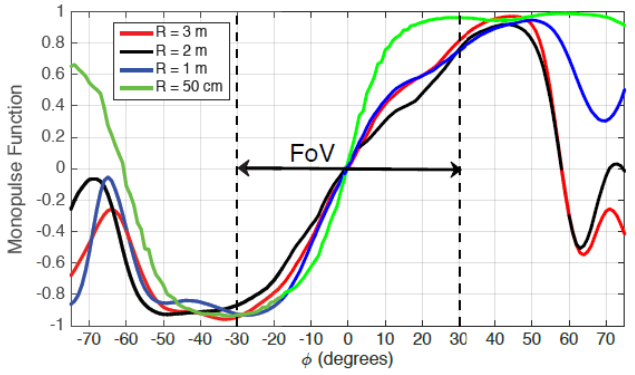

FIGURE 7. Measured monopulse functions as a function of ranging distance R after calibration of the monopulse offset.

Once the sum $\Sigma(\phi, R)$ and difference $\Delta(\phi, R)$ patterns, together with the monopulse correction factor $K_D(R)$, have been characterized in the anechoic chamber, the angular and range dependent monopulse functions $\Psi(\phi, R)$ (equation (4)) shown in Fig.7, are calibrated and recorded as summarized in the calibration process depicted in Fig.4. As explained in [35], the monopulse function shows an angular range without ambiguity, where it monotonically varies between -1 and $+1$, and which determines the FoV. As it can be seen in Fig.7, in our case the FoV is limited from $\phi = -30°$ to $\phi = +30°$. Within this FoV, both the AoA and the RTT ranging distance can be accurately estimated. Out from this FoV, the AoA estimation suffers from ambiguities, and as it was shown in Fig.5, the RTT-based ranging also shows increased error in the distance estimation.

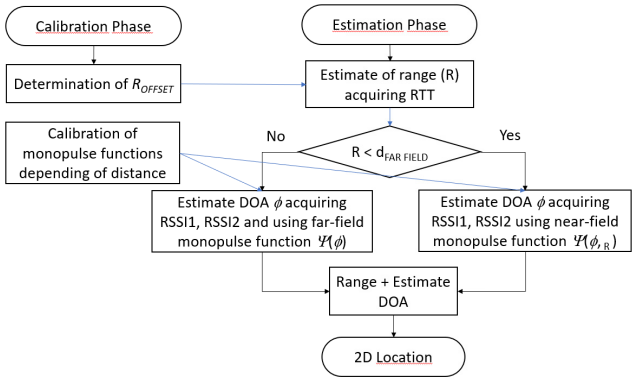

FIGURE 8. Flow-chart for ranging and AoA estimation process after calibration.

After the calibration phase, the estimation of the ranging distance R and the AoA angle ϕ, is accomplished by the algorithm sketched in Fig.8. First, the range R is estimated using the RTT FTM technique with the calibrated offset R_{OFFSET}. Once R is estimated, the AoA angle ϕ is estimated using the adequate monopulse function for this value of R. In particular, if R < 2.5m (which is the near-field distance) the pre-recorded monopulse function $\Psi(\phi, R)$ must be applied. If the estimated range R extends further into the far-field zone, then the far-field monopulse function $\Psi(\phi, R = 3m)$ can be used independently of the estimated distance.

As an example, the RTT range R and the AoA angle ϕ are estimated inside the anechoic chamber for different distances R, and the range and angular estimation error is plotted in Fig.9. As it was previously anticipated, the RTT-based distance estimation works better for larger distances and for angles within the FoV, showing an error below 10 cm for R $= 3$m and R $= 2$m and for angles between $\phi = -30°$ and $\phi = +30°$. For a shorter distance of R $= 1$m, this error increases up to 30cm and up to 60cm for R $= 50$cm, due to the aforementioned near-field inaccuracies.

Similarly, the AoA estimation shows an error below 5° inside this FoV $\phi = \pm 30°$ and for distances above R $= 1$m. For R $= 50$cm, the near-field effects involves a higher error in the AoA estimation, up to 20° even within this FoV (see Fig.9d). In any case, out of the FoV, both range and AoA estimation present increased inaccuracies. The AoA estimation error increases up to 60° for angles well far from the FoV (see for instance $\phi = \pm 70°$), and similarly the RTT-based distance estimation reaches error values up to 75cm. The increased AoA estimation error outside the FoV is mainly due to the fact that the monopulse function has a bi-univocal behavior only in the linear zone ranging from $-30°$ to $+30°$, as clearly shown in Fig.7 [16]. Outside this limited FoV, the AoA cannot be univocally guessed, leading to wrong angular estimates. Similarly, the RTT-based distance estimation performs better inside the FoV, where the panel antenna gain is greater. The FoV could be extended using scanning antennas, at the

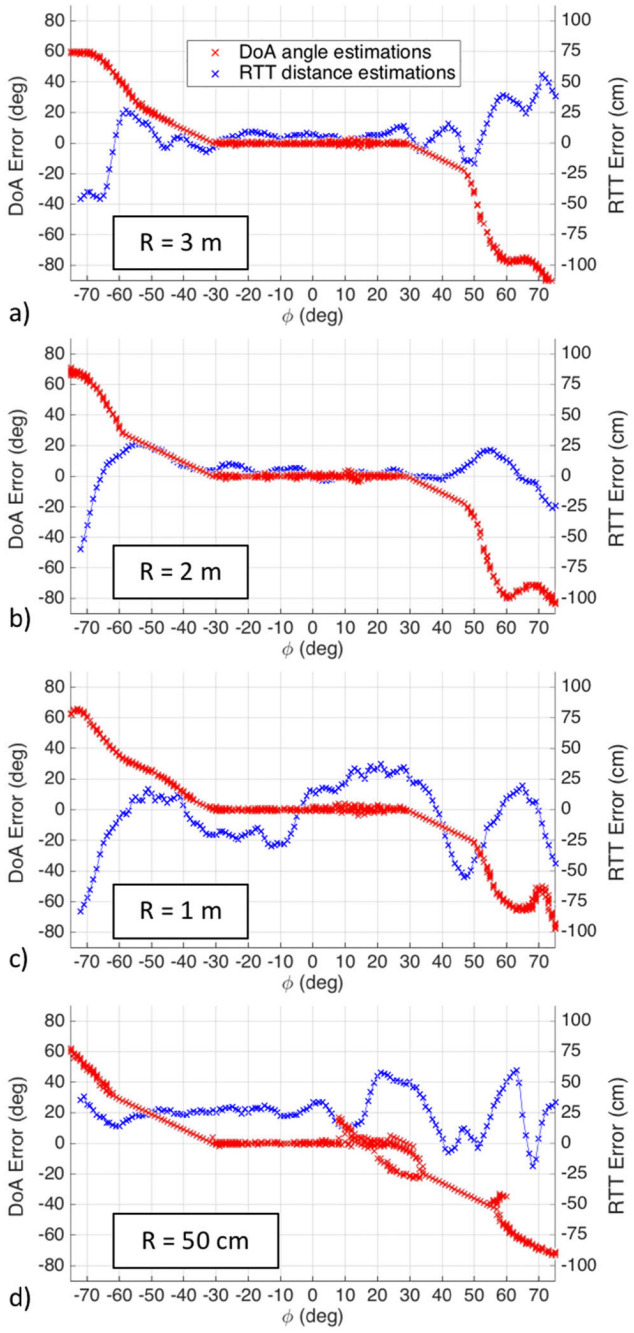

FIGURE 9. Ranging and angular estimation error in anechoic chamber for different radial distances a) R = 3 m b) R = 2 m c) R = 1 m d) R = 50 cm.

expense of a more complex system which is out of the scope of this work. As described in [35], thanks to the correct guess of the near-field distance, the appropriate dependent monopulse function can be chosen and the AoA estimation error due to near-field effects can be strongly mitigated. This makes this localization system suitable to localize mobile devices at distances even when the far-field radiation zone is not guaranteed. This is of much importance for real WLAN scenarios, where the mobile devices can be located at short distances from the Wi-Fi AP.

The performance of this single-AP Wi-Fi RADAR system for two-dimensional localization in a real outdoor scenario is evaluated in the following Section.

IV. TWO-DIMENSIONAL LOCALIZATION

Once calibrated, the single-AP RTT Wi-Fi monopulse RADAR has been placed in an outdoor scenario to evaluate its performance for real-time two-dimensional localization of 802.11mc compatible mobile devices. A total area of 12 m × 12 m is studied, using the 62cm × 70cm floor tiles as a grid. This is sketched in the pictures of Fig.10, leading to a total of 304 sampling points. The AP is located at x = 0 m y = 0 m, and for each sampling position with known coordinates, its distance R to the AP and its bearing angle ϕ are estimated to evaluate the two-dimensional positioning accuracy.

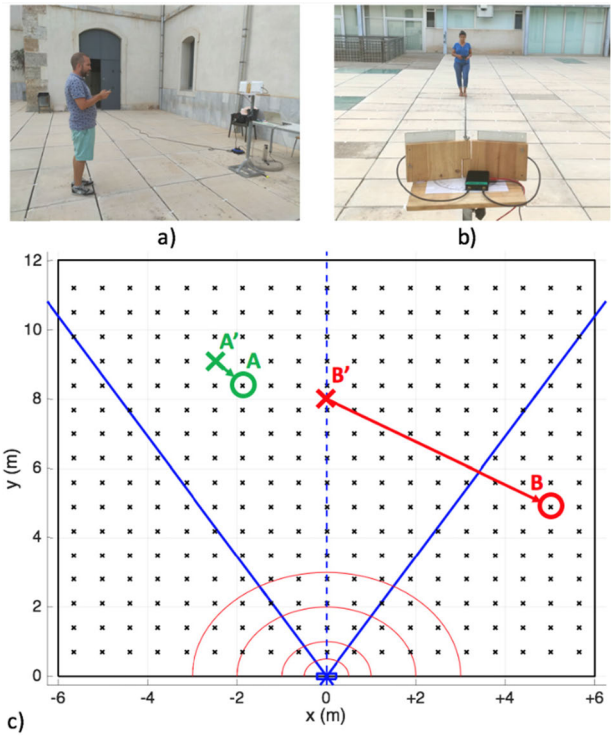

FIGURE 10. Experimental setup for outdoors localization with single-AP Wi-Fi RTT monopulse RADAR. a) Lateral view b) Front view c) Localization zone layout.

The blue lines in Fig.10c represent the limits of the angular FoV (from $\phi = -30°$ to $\phi = +30°$), while the red circles with radii R = 0.5m, R = 1m, R = 2m, and R = 3m show the near-field zones of the RADAR system. To illustrate the real-time signal processing for localization, the data acquired during 45 seconds are analyzed for two illustrative positions of the mobile devices: point A inside the FoV and point B outside the FoV. The sampling rate is 450 milisecs, so that a total of 100 samples are plotted in the 45 sec-long datagrams shown in Fig.11 and Fig.12 (for points A and B, respectively).

In Fig.10c, point A is located at coordinates x = − 1.875m, y = 8.4m, which corresponds to R = 8.6m and $\phi = -12.6°$

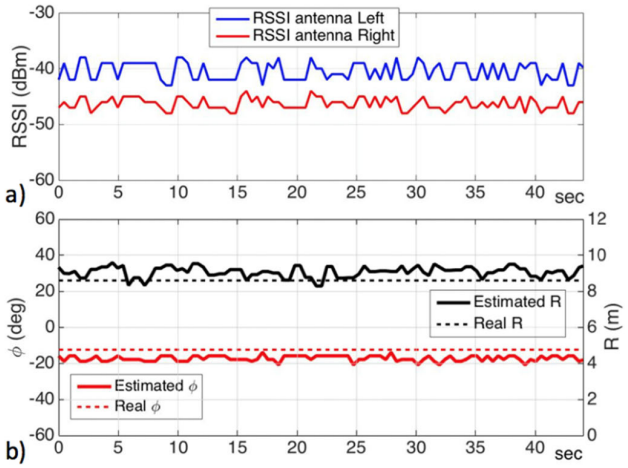

FIGURE 11. a) Real-time Wi-Fi signal acquisition and b) RADAR estimation inside the FoV (point A in Fig.10c).

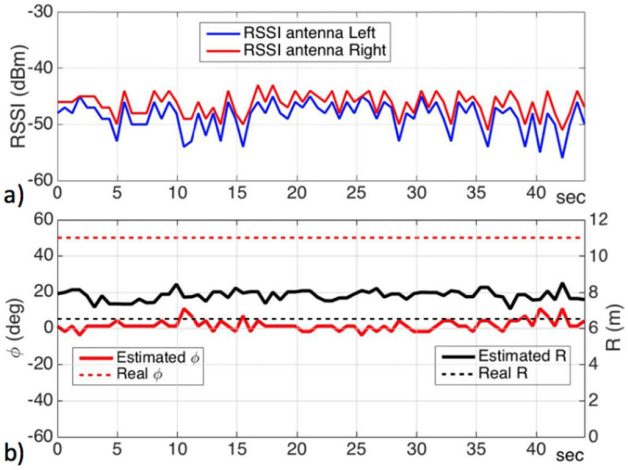

FIGURE 12. a) Real-time Wi-Fi signal acquisition and b) RADAR estimation outside the FoV (point B in Fig.10c).

inside the FoV. Fig.11a plots the RSSI acquired by each antenna connected to the MIMO Wi-Fi AP. As commented, every 450 msecs., the RSSI values are refreshed and processed in real-time using the amplitude monopulse technique to estimate the azimuthal AoA angle ϕ. Prior to that, the ranging distance R must first be estimated, to determine if the mobile is in the near-field or the far-field zone of the RADAR. The estimated distance R is plotted with continuous black line in Fig.11b, showing that it fluctuates above the real distance R = 8.6m (dashed black line), with a maximum deviation to R = 9.5m (this is, less than one meter error). Once the ranging distance is estimated, the location algorithm selects the appropriate monopulse function to estimate the AoA, as it was sketched in Fig.8. In this case, point A is in the far-field zone of the RADAR (R > 2.5m), so that the far-field monopulse function $\Psi(\phi, R = 3m)$ is applied to estimate ϕ from the acquired RSSI data at each antenna. The estimated AoA is plotted with continuous red line in Fig.11b, and it is compared to the real AoA $\phi = -12.6°$ (dashed red line).

In this case, since the point A is within the FoV, the estimated AoA shown in Fig.11b varies between $\phi = -14°$ and $\phi = -20°$, i.e. with a maximum error of 8° compared to the real AoA. It is remarkable that, despite the 5 dB variations in the acquired RSSI levels observed in Fig.11a, the estimated angle keeps stable with only this 6° fluctuation. As it can be seen in Fig.11a, the variations in the RSSI levels acquired from antenna left and antenna right are correlated. As it was explained in [16], the amplitude monopulse comparison technique absorbs the fluctuations due to fading, orientation, obstacles, etc. which affect similarly to both antennas, and which are not associated with a real AoA change.

The signals acquired for the point B, located at x = + 5m, y = 4.9m with R = 6.5m and $\phi = +50°$ outside the FoV, are analyzed in Fig.12. This time, both the estimation of distance and AoA suffer from higher errors. Particularly, the RTT FTM technique shows a mean error of 1.5m, estimating the distance around R = 8m. More remarkable is the AoA estimation error, which due to ambiguities outside the FoV estimates a false AoA around the perpendicular direction of the AP $\phi = 0°$, leading to wrong location of the mobile device as shown by the point B' in Fig.10c.

To better illustrate the overall localization performance of the proposed RTT Wi-Fi monopulse RADAR system, the AoA estimation error, the ranging estimation error, and the eventual two-dimensional localization error (Euclidean distance error) are analyzed for the 304 sampling points covering the 12m × 12m testing grid. The spatial distribution of the error is plotted as a heatmap in Fig.13. In particular, Fig.13a illustrates the AoA error, showing that inside the FoV this error keeps below 10° in most of the points, while outside the FoV the monopulse ambiguities strongly increase the uncertainty in the estimation of the AoA angle. The range estimation plotted in Fig.13b also suffers from higher error outside the FoV, although this is not so remarkable as for the AoA estimation. As commented, close to the AP (R < 3m), the RTT ranging estimation error is higher due to the near-field effects. Also, for distances above 10m the RTT inaccuracy increases; therefore, at a mid-distance ranging between R = 3m and R = 10m the RTT precision shows the best ranging estimation.

In any case, once the ranging R and the AoA angle ϕ have been estimated, the two-dimensional coordinates {x,y} of the mobile device can be calculated. The Euclidean distance between the real location and the estimated coordinates is evaluated for each point, and the resulting spatial distribution of the localization error is plotted in Fig.13c. It is clearly distinguible the difference in the performance inside and outside the FoV. The Cumulative Distribution Function (CDF) for each estimate (AoA, ranging, and Euclidean distance errors) is plotted in Fig.14 to summarize the system performance, distinguing between inside the FoV, outside the FoV, and the whole zone performance.

Fig.14a illustrate the distribution of the CFD for the AoA error obtained from the monopulse function. It is demonstrated that 90% of the samples inside the FoV show less than

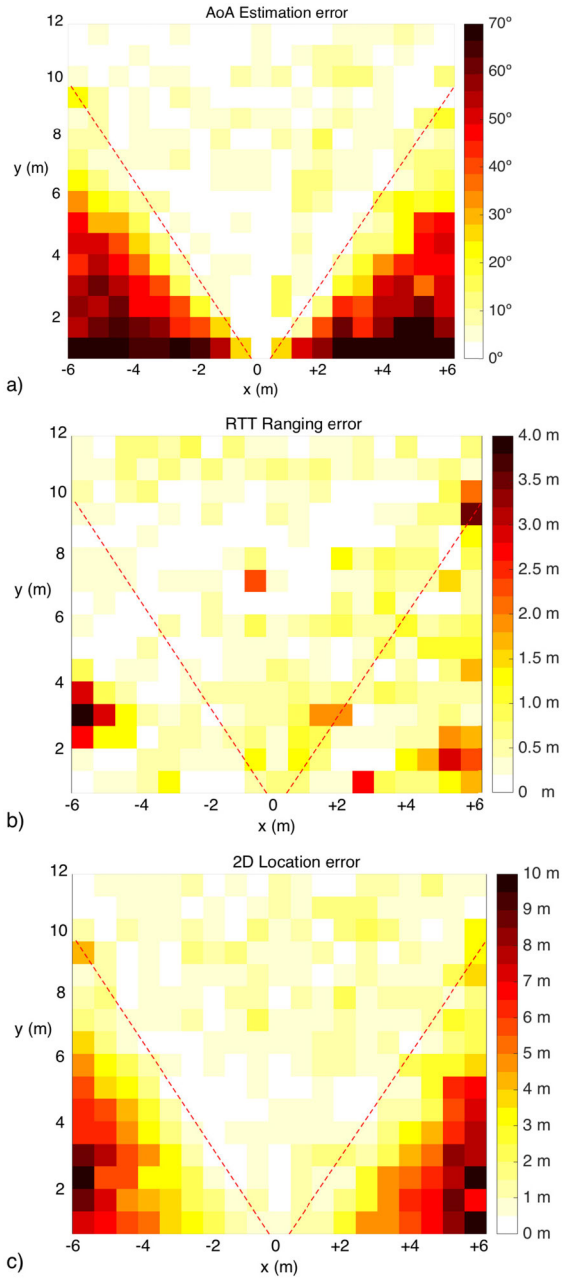

FIGURE 13. Spatial distribution of mean error in the estimation of a) angle of arrival ϕ, b) range distance R, and c) 2D location.

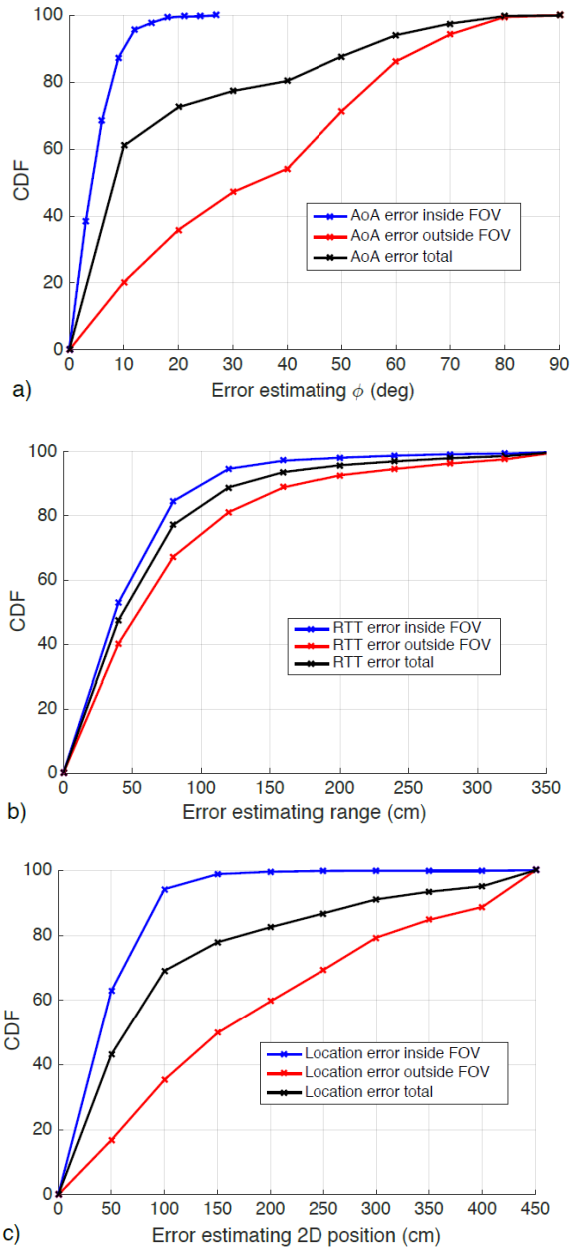

FIGURE 14. CDF for estimation error of a) angle of arrival ϕ, b) range distance R, and c) 2D location.

10° AoA estimation error, and 100% of the samples present an error below 28°. As summarized in Table 2, the corresponding root mean square error (RMSE) is below 6° and the mean error is below 5° for this FoV zone. Outside the FoV, the AoA estimation strongly deteriorates, reporting a 90% percentile with almost 65° error and 34° mean angular error. The CDF with the ranging errors measured from the RTT distance estimation is shown in Fig.14b, reporting a 90% percentile of the samples inside the FoV with less than 1 meter deviation from their actual distance to the Wi-Fi AP. This ranging error 90% percentile increases up to 170cm outside the FoV. As previously commented, the ranging estimation performance does not deteriorate so much out of the FoV zone, as it happened to the AoA estimation.

This is evident from the CDF curves, which show that the AoA CDF strongly worses outside the FoV in Fig14a, while the RTT CDF in Fig.14b keeps more stable although pointing out higher error outside the FoV. The associated RMSE and mean ranging error are summarized in Table 3, showing that inside the FoV the mean error is below 50cm, while outside the FoV it increases to 77cm.

Finally, the two-dimensional localization performance with the combination of monopulse function and the

TABLE 2. Angular Errors From Monopulse Estimation.

Zone	RMSE	Mean error	90% percentile
Inside FoV	5.89º	4.66º	9.6º
Outside FoV	40.75º	33.97º	64.9º
Total	27.02º	17.19º	53.38º

TABLE 3. Ranging Errors From RTT Estimation.

Zone	RMSE	Mean error	90% percentile
Inside FoV	71.83 cm	48.47 cm	94.17 cm
Outside FoV	113.67 cm	77.13 cm	169.72 cm
Total	92.1 cm	60.72 cm	128.14 cm

TABLE 4. Euclidean Distance Error From Two-Dimensional Location Estimation.

Zone	RMSE	Mean error	90% percentile
Inside FoV	115.85 cm	94.94 cm	171.47 cm
Outside FoV	446.48 cm	363.6 cm	747.53 cm
Total	304.84 cm	209.82 cm	572.35 cm

ranging measured with RTT is summarized in Table 4 and the associated CDF curves are plotted in Fig.14c. Due to the strong influence of the FoV zone in the AoA estimation, the resulting localization performance also reports a strong degradation outside the FoV, as it can be seen in the corresponding CDF curves in Fig.14c. As summarized in Table 4, 90% of the samples inside the FoV can be localized with 1.7m of error, leading to a mean error below 1 meter inside the vision of the Wi-Fi RADAR. Outside the FoV, the localization error strongly increases above 3.5m, mainly due to the AoA ambiguities. This limited 60° FoV without ambiguities can be increased using beam-scanning monopulse antennas [36], like the one proposed for Bluetooth Low Energy (BLE) localization systems [37].

Therefore, we can conclude that the proposed RTT Wi-Fi monopulse RADAR system provides a mean positioning error below one meter within a Field of View of 60° and distances up to 14 meters. Thanks to the adaptative range-dependent monopulse functions, the localization system can successfully operate also in the near-field zone of the AP, which for Wi-Fi frequencies extends up to 3 meters from the monopulse antennas. Moreover, due to the directly accessible RTT and RSSI data, real-time operation with an acquisition and processing time below 0.5 seconds is demonstrated using a single 802.11mc MIMO Wi-Fi Access Point and FTM-compatible mobile devices. A single commercial AP has been used, without the need of modifying the hardware and/or software to acquire complex CSI / IQ data to obtain Time-of-Fligth information. The next Section compares the proposed RTT Wi-Fi monopulse system with other state-of-the-art single-AP Wi-Fi real-time localization systems (RTLS).

V. COMPARISON WITH OTHER SINGLE AP WI-FI RTLS

As depicted in the introduction section, some works about a single-AP localization systems have already been published. As will be detailed below, most of them require complex processing techniques employing the CSI information or the use of channel hopping mechanism out of the Wi-Fi standard. In the next paragraph and in Table 5, we will describe the information employed in each of the already published single AP system together with the main differences with our system.

CUPID [23] was the first paper published under these premises. Like many other proposals enumerated later, the algorithms require access to the transmission's CSI information. This operation cannot be performed in most of the off-the-shelf AP. Therefore, in the demonstration experiments, the authors do not use a commercial AP. Indeed, they use a laptop with an external Wi-Fi card as an AP, and simulate an IoT device to be localized with another laptop. This is because the system required a modification in the device's PHY layer which is not accesible in commercial smartphones. Moreover, the laptot working as receiver has to run specific tools for accessing the CSI data of the transmission and receive the information of the smartphone's inertial sensors simultaneously. The mean error localization value of this system is around 5 meters.

On the contrary to CUPID [23], the SAIL [24] proposal employed a commercial AP. However, an internal 88MHz WLAN clock is required to compute the Time-of-Flight (ToF) based on Time-of-Departure (ToD) and Time-of-Arrival (ToA) from the PHY layer. This precise clock is not present in commercial Wi-Fi cards. Moreover, the calculation of ToF requires computing the CIR (Channel Impulse Response) from CSI information and the use of dead reckoning system employing the inertial sensor from the smartphone. The reported mean localization error of SAIL is 2.5 meters.

One of the most accurate systems is Chronos [25], with a few decimeters of error in Line-Of-Sight conditions. Chronos implements a channel-hopping mechanism among 35 Wi-Fi channels to estimate the ToF. Since this channel-hopping procedure is out of the Wi-Fi standard, Chronos was implemented into a driver modification and tested with two PCs which must synchronize the frequency band in each hopping with a periodicity of 2-3 msec.

Another channel-hopping proposal is S-Phaser [26]. This system, similar to those above, requires access to CSI information and synchronization algorithms for estimating the distances. The authors proposed a synchronization algorithm for resolving the errors in the phase estimation reading the CSI and computing a precise ranging system, and another algorithm for the ranging estimation. For the testing procedure, a PC was employed to access the CSI information with 1.5 meters of accuracy in Line-Of-Sight (LoS) conditions.

Splicer [28] is another channel hopping approach which integrates a splicing mechanism for aggregating the CSI acquired in different frequencies. This work generated a power delay profile, which was used for computing the ranging to the devices. Some processing techniques are required to remove the amplitude and phase errors introduced by the hardware. The mean error obtained by this works is around 1 meter.

TABLE 5. Comparative Table With Other Single AP Location System.

	Main Characteristics	Problems	Mean Error
Cupid [23]	Ranging and AoA computed accessing the CSI and a inertial sensors from smartphone	The device to locate must have inertial sensors from smartphone.	Around 5 m
Sail [24]	ToF solution employing the CIR from the PHY layer and internal clock of Wi-Fi cards	Needs for a very precise internal Wi-Fi card clock not present in all commercial hardware	2.5 m
Chronos [25]	ToF obtained from CSI with 35 Wi-Fi channel hopping	Requires driver modification out of Wi-Fi standard for channel hopping	Decimeters in LoS
S-Phaser [26]	Ranging system from CSI with two Wi-Fi channels hopping and three MIMO antennas triangulation	Requires driver modification out of Wi-Fi standard for channel hopping	1.5 m in LoS
SiFi [27]	ToF triangulation system based on three MIMO antennas using CSI, and separated from the AP a few meters	Cannot be employed in real-time because the high complexity	0.93 m
Splicer [28]	Power delay profiling with a mechanism for correct the hardware CSI error	Requires driver modification out of Wi-Fi standard for channel hopping	1 m
[29]	Switched Beam Antenna with eight directional antenna	Employs a complex antenna system which must be electronically controlled	0.95 m in anechoic chamber
[30]	Bluetooth RSSI data and motion sensors	The device must have inertial sensors	5.6 m
Proposed method	2D radar with RTT and RSSI-based monopulse antenna	Only cover 60º of FoV	0.95 m

A localization system with a single AP and without channel hopping is SiFi [27]. This work is a ToF one channel system which requires three antennas installed far away from the AP. With the simultaneous access to the CSI from the three antennas, authors can estimate the direct path from the transmitter to each antenna and estimate the delay time. With that information and triangulation, the system achieved an accurate position. The system is tested with a PC with the Linux CSI Tool working as an AP and another PC as the target to localize. The antenna connected to the AP has to be installed several meters away from the PC, and it is a handicap of the system. Additional drawbacks of the system are the high computation complexity which avoids the real-time localization implementation and the limitation of localizing only one user per time. The mean error of SiFi is 0.93 meters.

Similar to our proposal regarding the use of RSSI values without requiring CSI accessing is [29]. However, in this proposal, a complex eight dual 2.4 - 5GHz Switched Beam Antenna designed explicitly for this proposal is required. These antennas must be electronically switched on and off. Our proposal works with RSSI similar to this last one, but on the contrary, only two tiled commercial directive antennas are employed using a commercial 2×2 MIMO Wi-Fi card which can read the RSSI from each titled antenna. Moreover, the mean error reported in [29] is about 1 meter in an anechoic chamber with optimum propagation conditions, and no information is given about its operating real-time performance outside the anechoic chamber. Another RSSI-based single-AP RTLS was proposed in [30]. In this work and similar to [23], [24], because of the limitation of estimating the position employing only a unique AP, a dead reckoning system in the smartphone was implemented using the inertial sensors of the mobile IoT device.

To the authors' knowledge, the proposed RTT Wi-Fi monopulse system is the first single-AP system that can precisely localize an IoT device without the use of complex signal processing techniques, neither the use of CSI information nor the smartphone inertial system. Only with the use of the RSSI and RTT data directly accessible from commercial 802.11mc MIMO Wi-Fi Access Point, the proposed system is able to estimate the AoA angle and the ranging distance of any 802.11mc-compatible IoT device. With both the angle and the distance, the precise position can be easily determined. Moreover, because of the easy-to-acquire and low-cost complexity, the system is able to localize in real-time and more than one device simultaneously, using a single commercial AP.

VI. CONCLUSION

It has been demonstrated that a single commercial 802.11mc MIMO Wi-Fi Access Point connected to a monopulse antenna, can be successfully used to estimate the Direction-of-Arrival and the ranging distance to a mobile IoT device, without the need of accesing complex CSI data, which relies on non-standard synchronization process (which requests specific hardware and software out of the IEEE WiFi standard to perform the time and/or phase synchronization for precise CSI-based localization). The directly accessible RSSI and RTT information provided by any commercial 802.11mc MIMO Wi-Fi AP is sufficient to perform the two-dimensional localization, thus allowing real-time operation with commercial mobile IoT devices, and without the need of using inertial sensors. It is reported a positioning error below 1 meter, with an acquisition and processing time below 0.5 seconds. Its main drawback is that this succesful performance deteriorates out of the limited monopulse antenna Field of View of 60°, due to angular ambiguities. This limitation can be improved using several APs, or using beam-scanning monopulse systems, at the cost of increasing the overall system complexity. In any case, the demonstrated single-AP real-time

localization performance inside this 60° FoV, together with its relative simplicity, makes this Wi-Fi RTLS an interesting solution for low-cost commercial applications using the 802.11mc FTM protocol for RTT ranging, together with RSSI-based angular monopulse techniques.

In future research we will study the potential localization system improvement when several APs are employed, or when beam-scanning monopulse antennas are used to extend the limited FoV

ACKNOWLEDGMENT

The authors would like to thank Neuromobile and CENTIC for their support.

REFERENCES

[1] F. Khelifi, A. Bradai, A. Benslimane, P. Rawat, and M. Atri, "A survey of localization systems in Internet of Things," *Mobile Netw. Appl.*, vol. 24, no. 3, pp. 761–785, Jun. 2019.

[2] F. Liu, J. Liu, Y. Yin, W. Wang, D. Hu, P. Chen, and Q. Niu, "Survey on WiFi-based indoor positioning techniques," *IET Commun.*, vol. 14, no. 9, pp. 1372–1383, Jun. 2020.

[3] S. He and S.-H.-G. Chan, "Wi-Fi fingerprint-based indoor positioning: Recent advances and comparisons," *IEEE Commun. Surveys Tuts.*, vol. 18, no. 1, pp. 466–490, 1st Quart., 2016.

[4] M. Youssef and A. Agrawala, "The horus WLAN location determination system," in *Proc. 3rd Int. Conf. Mobile Syst., Appl., Services (MobiSys)*, 2005, p. 205.

[5] Z. Guowei, X. Zhan, and L. Dan, "Research and improvement on indoor localization based on RSSI fingerprint database and K-nearest neighbor points," in *Proc. Int. Conf. Commun., Circuits Syst. (ICCCAS)*, Nov. 2013, vol. 2, no. 3, pp. 68–71.

[6] D. Han, S. Jung, M. Lee, and G. Yoon, "Building a practical Wi-Fi-based indoor navigation system," *IEEE Pervasive Comput.*, vol. 13, no. 2, pp. 72–79, Apr./Jun. 2014.

[7] J. A. Lopez-Pastor, A. J. Ruiz-Ruiz, A. S. Martinez-Sala, and J. L. Gomez-Tornero, "Evaluation of an indoor positioning system for added-value services in a mall," in *Proc. Int. Conf. Indoor Positioning Indoor Navigat. (IPIN)*, Sep. 2019, pp. 1–8.

[8] P. Bahl and V. N. Padmanabhan, "RADAR: An in-building RF-based user location and tracking system," in *Proc. IEEE INFOCOM Conf. Comput. Commun. 19th Annu. Joint Conf. IEEE Comput. Commun. Societies*, 2000, pp. 775–784.

[9] W. Li, Y. Chen, and M. Asif, "A Wi-Fi-based indoor positioning algorithm with mitigating the influence of NLOS," in *Proc. 8th IEEE Int. Conf. Commun. Softw. Netw. (ICCSN)*, Jun. 2016, pp. 520–523.

[10] J. Xiong, K. Sundaresan, and K. Jamieson, "ToneTrack: Leveraging frequency-agile radios for time-based indoor wireless localization," in *Proc. 21st Annu. Int. Conf. Mobile Comput. Netw.*, Sep. 2015, pp. 537–549.

[11] S. Aditya, A. F. Molisch, and H. M. Behairy, "A survey on the impact of multipath on wideband time-of-arrival based localization," *Proc. IEEE*, vol. 106, no. 7, pp. 1183–1203, Jul. 2018.

[12] J. Xiong and K. Jamieson, "ArrayTrack: A fine-grained indoor location system," in *Proc. USENIX Symp. Netw. Syst. Des. Implement.*, no. 279976, 2013, pp. 71–84.

[13] R. O. Schmidt, "Multiple emitter location and signal parameter estimation," *Adapt. Antennas Wireless Commun.*, no. 3, pp. 190–194, 2009.

[14] R. Roy, A. Paulraj, and T. Kailath, "ESPRIT—A subspace rotation approach to estimation of parameters of cisoids in noise," *IEEE Trans. Acoust., Speech, Signal Process.*, vol. ASSP-34, no. 5, pp. 1340–1342, Oct. 1986.

[15] S. Maddio, A. Cidronali, and G. Manes, "RSSI/AoA based positioning systems for wireless sensor network," in *New Approach Indoor Outdoor Localization Systems*. IntechOpen, 2012, ch. 7.

[16] J. L. Gómez-Tornero, D. Cañete-Rebenaque, J. A. López-Pastor, and A. S. Martínez-Sala, "Hybrid analog-digital processing system for amplitude-monopulse RSSI-based MIMO WiFi direction-of-arrival estimation," *IEEE J. Sel. Topics Signal Process.*, vol. 12, no. 3, pp. 529–540, Jun. 2018.

[17] *IEEE Standard for Information Technology—Telecommunications and Information Exchange Between Systems Local and Metropolitan Area Networks—Specific Requirements—Part 11: Wireless LAN Medium Access Control (MAC) and Physical Layer*, IEEE Standard 802.11-2016, 2016. Accessed: Dec. 11, 2020. [Online]. Available: https://standards.ieee.org/standard/802_11-2016.html

[18] *Wi-Fi Location: Ranging With RTT*. Accessed: Dec. 11, 2020. [Online]. Available: https://developer.android.com/guide/topics/connectivity/wifi-rtt

[19] M. Ibrahim, H. Liu, M. Jawahar, V. Nguyen, M. Gruteser, R. E. Howard, B. Yu, and F. Bai, "Verification: Accuracy evaluation of WiFi fine time measurements on an open platform," in *Proc. 24th Annu. Int. Conf. Mobile Comput. Netw. (MobiCom)*, 2018, pp. 417–427.

[20] S. Xu, R. Chen, Y. Yu, G. Guo, and L. Huang, "Locating smartphones indoors using built-in sensors and Wi-Fi ranging with an enhanced particle filter," *IEEE Access*, vol. 7, pp. 95140–95153, 2019.

[21] Y. Yu, R. Chen, L. Chen, S. Xu, W. Li, Y. Wu, and H. Zhou, "Precise 3-D indoor localization based on Wi-Fi FTM and built-in sensors," *IEEE Internet Things J.*, vol. 7, no. 12, pp. 11753–11765, Dec. 2020.

[22] H. Jiang, C. Cai, X. Ma, Y. Yang, and J. Liu, "Smart home based on WiFi sensing: A survey," *IEEE Access*, vol. 6, pp. 13317–13325, 2018.

[23] S. Sen, J. Lee, K.-H. Kim, and P. Congdon, "Avoiding multipath to revive inbuilding WiFi localization," in *Proc. 11th Annu. Int. Conf. Mobile Syst., Appl., Services (MobiSys)*, 2013, p. 249.

[24] A. T. Mariakakis, S. Sen, J. Lee, and K.-H. Kim, "SAIL: Single access point-based indoor localization," in *Proc. 12th Annu. Int. Conf. Mobile Syst., Appl., Services*, Jun. 2014, pp. 315–328.

[25] D. Vasisht, S. Kumar, and D. Katabi, "Decimeter-level localization with a single WiFi access point," in *Proc. 13th USENIX Symp. Netw. Syst. Design Implement. (NSDI)*, 2016, pp. 165–178.

[26] S. Han, Y. Li, W. Meng, C. Li, T. Liu, and Y. Zhang, "Indoor localization with a single Wi-Fi access point based on OFDM-MIMO," *IEEE Syst. J.*, vol. 13, no. 1, pp. 964–972, Mar. 2019.

[27] W. Gong and J. Liu, "SiFi: Pushing the limit of time-based WiFi localization using a single commodity access point," *Proc. ACM Interact., Mobile, Wearable Ubiquitous Technol.*, vol. 2, no. 1, pp. 1–21, 2018.

[28] Y. Xie, Z. Li, and M. Li, "Precise power delay profiling with commodity Wi-Fi," *IEEE Trans. Mobile Comput.*, vol. 18, no. 6, pp. 1342–1355, Jun. 2019.

[29] M. Passafiume, S. Maddio, G. Collodi, and A. Cidronali, "An enhanced algorithm for 2D indoor localization on single anchor RSSI-based positioning systems," in *Proc. Eur. Radar Conf. (EURAD)*, Oct. 2017, pp. 287–290.

[30] Y. Li, Z. He, Y. Li, Z. Gao, R. Chen, and N. El-sheimy, "Cost-effective localization using RSS from single wireless access point," *IEEE Trans. Instrum. Meas.*, vol. 69, no. 5, May 2020, Art. no. 41804027.

[31] S. M. Sherman and D. K. Barton, *Monopulse Principles and Techniques* (Artech House Radar Library), 2nd ed. Norwood, MA, USA: Artech House, 2013.

[32] S. Gogineni and A. Nehorai, "Monopulse MIMO radar for target tracking," *IEEE Trans. Aerosp. Electron. Syst.*, vol. 47, no. 1, pp. 755–768, Jan. 2011.

[33] *Yocto Indoor Positioning Evaluation Kit*. Accessed: Nov. 13, 2020. [Online]. Available: https://fit-iot.com/web/product/indoor-positioning-evaluation-kit/

[34] *Interline 14 dB Panel Antenna IP-G14-F2425-H, Datasheet*. Accessed: Nov. 13, 2020. [Online]. Available: http://www.interline.pl/antennas/PANEL-14-2.4GHz

[35] J. A. López-Pastor, A. Gómez-Alcaraz, D. Cañete-Rebenaque, A. S. Martínez-Sala, and J. L. Gómez-Tornero, "Near-field monopulse AoA estimation for angle-sensitive proximity WiFi readers," *IEEE Access*, vol. 7, no. 1, pp. 88450–88460, Jun. 2019.

[36] M. Poveda-García, D. Cañete-Rebenaque and J. L. Gómez-Tornero, "Frequency-scanned monopulse pattern synthesis using leaky-wave antennas for enhanced power-based direction-of-arrival estimation," *IEEE Trans. Antennas Propag.*, vol. 67, no. 11, pp. 7071–7086, Nov. 2019.

[37] M. Poveda-García, A. Gómez-Alcaraz, D. A. S. Cañete-Rebenaque Martínez-Sala, and J. L. Gómez-Tornero, "RSSI-based direction-of-departure estimation in Bluetooth low energy using an array of frequency-steered leaky-wave antennas," *IEEE Access*, vol. 8, pp. 9380–9394, Jan. 2020.

JOSÉ ANTONIO LÓPEZ-PASTOR (Graduate Student Member, IEEE) received the B.S. degree in telematics engineering and the M.S. degree in telecommunication engineering from the Universidad Politecnica de Cartagena (UPCT), Cartagena, Spain, in 2006 and 2010, respectively. He is currently pursuing the Ph.D. degree with the Technical University of Cartagena (UPCT). He was with private Research and Development Technological Center for 8 years. He also a Researcher with SL (Neuromobile) company. His research interests include indoor positioning systems, software programming, and the IoT.

PEDRO ARQUES-LARA received the bachelor's degree in telecommunication engineering from the Polytechnic University of Cataluña (UPC), in 1995. He has also conducted technical consultancies for several large companies, Mid-Caps and SMEs in the TELCO sector. He has worked mainly as Project Manager since 2000 and has successfully participated as a technical advisor and an evaluator in several Research and Development projects and initiatives in the ICT area under the EU H2020 program. As an engineer, he worked for 10 years with Alcatel-Lucent Technologies (Bell Labs Innovations), Madrid, from 1998 to 2008. He has been a member of Project Management Institute (PMI) and responsible of Quality Assurance with the NPS Lab Unit. Since 2008, he has been a Project Manager and a Research and Development Consultant with CENTIC, an ICT private Research Technical Organization (RTO), Murcia. He is currently a telecommunications engineer with more than 25 years of experience in the operational and executive management of ICT technologies, deployments, and services. He holds a practical experience in network planning, bid and proposals and overseas international projects. He has coauthored the published article *Drones, ecall and cyber physical systems for public safety: answering points 112* at ECSA '18 and *Proceedings of the 12th European Conference on Software Architecture* (Madrid: September 2018). He has been titled as a Distinguished Member of Technical Staff (DCMS) during his working period in Lucent Technologies.

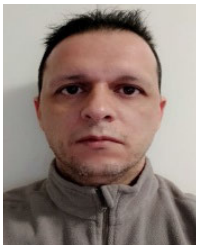

JUAN JOSÉ FRANCO-PEÑARANDA was born in Murcia, Spain, in 1981. He received the bachelor's degree in computer science from the University San Jorge of Zaragoza (USJ), in 2010, and the master's degree in development of applications for mobile devices from the Open University of Cataluña (UOC), in 2018. He is currently pursuing the industrial Ph.D. degree with the Catholic University of Murcia (UCAM). As a Software Engineer, he works in IoT projects with the CENTIC, Murcia.

ANTONIO JAVIER GARCÍA-SÁNCHEZ received the bachelor's degree in industrial electronic engineering and the master's degree in industrial engineering from the Technical University of Cartagena (UPCT), Spain, in 1997 and 2000, respectively, and the Ph.D. degree from UPCT, in 2005. As an Industrial Engineer, he worked in public and private entities such as the Centro de Desarrollo Tecnológico Industrial (CDTI-2000/01), in the technical evaluation of R+D+i projects of the national productive business sector. In 2001, he was the Head of maintenance with the Factory of Cartagena, Fertiberia S.A. Since 2002, he has been with the Information and Communication Technologies Department (DICT), UPCT. He has been a Visiting Scholar with Bologna University, Italy, in 2007; Wageningen University, The Netherlands, in 2012; and Cali University, Colombia, in 2019. Since July 2020, he has been a Co-Founder and a CTO of the spinoff QARTECH Innovations SL, dedicated to endow Industria 4.0 with high-performance technology. Since September 2020, he has been a Full Professor with ANECA. He is currently an Associate Professor of telematics engineering with UPCT and the Head of DICT. He has coauthored more than 100 international conferences and journal articles, 46 of them indexed in the Journal Citation Report (JCR), divided into 33 Q1, 7 Q2, 4 Q3, and 2 Q4. Furthermore, he has also published 12 international journals not indexed in JCR, and 29 IEEE/ACM conferences. He has led or leads five regional/national projects and six private contracts, ranging from fundamental research to those whose goal is to place on the consumer market devices, procedures, and tools. He has been responsible for a European H2020 project. In addition, he currently leads a project related to the COVID-19 area funded by CSIC and Banco Santander. In the field of technology transfer, he is a co-inventor of 14 patents/intellectual property (one of them USA), having been recognized by the Ministry of Science and Innovation a six-year transfer. He has more than 3.000 hours of teaching experience with high recognition by students (he was recognized as distinguished professor in 2019), thus including several teaching innovation projects. He is currently granted by two national research from 2003 to 2010 and from 2011 to 2016, one national transfer from 2002 to 2017, and three national teaching from 2002 to 2006, from 2007 to 2011, and from 2012 to 2016 recognitions. His current research interests include wireless sensor networks (WSNs) and the Internet of Things, streaming services, performance evaluation of communication networks, smart data processing, and nanocommunications. He has belonged to more than 35 conferences/workshops as TPC staff and to eight as a member of the organizing committee (IEEE/ACM conferences). He is a regular reviewer of notable communication journals listed in the ISI-JCR, highlighting the IEEE Internet of Things Journal, the IEEE Journal on Selected Areas in Communications, the IEEE Transactions on Industrial Electronics, the IEEE Transactions on Network and Service Management, *Computer Networks*, among others.

JOSÉ LUIS GÓMEZ-TORNERO (Senior Member, IEEE) was born in Murcia, Spain, in 1977. He received the degree in telecommunications engineering from the Technical University of Valencia, Valencia, Spain, in 2001, and the Ph.D. degree from the Technical University of Cartagena (UPCT), Cartagena, Spain, in 2005. He was the Vice Dean of students and Lectures affairs as a member of the Telecommunication Engineering Faculty. He has been a Visiting Researcher/Professor with the University of Loughborough, U.K.; Heriot-Watt University, Edinburgh, U.K.; Queen's University of Belfast, U.K. and CSIRO-ICT Centre, Sydney, NSW, Australia. In February 2010, he was appointed a CSIRO Distinguished Visiting Scientist by the CSIRO ICT Centre. In 2000, he joined the Radio Frequency Division, Industry Alcatel Espacio, Madrid, Spain. In 2001, he joined UPCT, where he has been an Associate Professor since 2008, and has also been a Full Professor since 2019. In August 2020, he was honorary appointed as a Visiting Professor with the University of Technology Sydney. He has coauthored more than 80 peer-reviewed journal articles, and more than 150 conference articles. His current research interests include the analysis and design of leaky-wave devices and their applications, and the innovation in the area of higher education.

Dr. Gómez-Tornero research work has received various awards, including EPSON-Ibérica foundation, in 2004, and Vodafone Foundation, in 2005, awards to the best Ph.D. thesis in the area of advanced mobile communications technologies, Hispasat, in 2014, and Hisdesat, in 2015, prizes to the best Ph.D. thesis in Satellite Communication technologies. Also, he was a co-recipient of the 2010 IEEE Engineering Education Conference Award, the 2011 EuCAP Best Student Paper Prize, the 2012 EuCAP Best Antenna Theory Paper Prize, the 2012 and 2013 Spanish URSI Prize for the best student paper, the 2013 APS Best Student Paper finalist, and the 2018 iWAT Best Poster award.